PROCEEDINGS B

Dual function of the pectoral girdle for feeding and locomotion in white-spotted bamboo sharks

Journal:	*Proceedings B*
Manuscript ID	RSPB-2017-0847.R1
Article Type:	Research
Date Submitted by the Author:	n/a
Complete List of Authors:	Camp, Ariel; Brown University, Ecology and Evolutionary Biology Scott, Bradley; University of Illinois at Urbana-Champaign College of Liberal Arts and Sciences, Dept. of Animal Biology Brainerd, Elizabeth; Brown University, Functional Morphology and Biomechanics Laboratory, Ecology and Evolutionary Biology Wilga, Cheryl; University of Alaska Anchorage, Dept. of Biological Sciences
Subject:	Biomechanics < BIOLOGY
Keywords:	XROMM, fluoromicrometry, scapulocoracoid, cranial elevation, skeletal kinematics, suction
Proceedings B category:	Morphology & Biomechanics

Title: Dual function of the pectoral girdle for feeding and locomotion in white-spotted bamboo sharks

Running Head: Dual function of the pectoral girdle

Authors: Ariel L. Camp*[1], Bradley Scott**[2], Elizabeth L. Brainerd[3], Cheryl D. Wilga[1,2]

Author Affiliations:

[1]Dept. of Biological Sciences, University of Alaska Anchorage, Anchorage, AK USA

[2]Dept. of Biological Sciences, University of Rhode Island, Kingston, RI USA

[3]Dept. of Ecology and Evolutionary Biology, Brown University, Providence, RI USA

*currently at Dept. of Ecology and Evolutionary Biology, Brown University, Providence, RI USA

**currently at Dept. of Animal Biology, University of Illinois, Champaign, IL USA

Contact Information for Corresponding Author:

Dept. of Ecology and Evolutionary Biology, Brown University, Providence, RI USA

ariel_camp@brown.edu

Keywords: XROMM, fluoromicrometry, scapulocoracoid, cranial elevation, skeletal kinematics, suction expansion

Word Count: 5185

Figures: 4

Tables: 1

Supplementary Materials: 1 Table, 2 Figures, 1 Video

Abstract

Positioned at the intersection of the head, body, and forelimb, the pectoral girdle has the potential to function in both feeding and locomotor behaviors—although the latter has been studied far more. In ray-finned fishes the pectoral girdle attaches directly to the skull and is retracted during suction feeding, enabling the ventral body muscles to power rapid mouth expansion. However in sharks, the pectoral girdle is displaced caudally and entirely separate from the skull (as in tetrapods), raising the question of whether it is mobile during suction feeding and contributing to suction expansion. We measured 3D kinematics of pectoral girdle in white-spotted bamboo sharks during suction feeding with X-ray Reconstruction of Moving Morphology (XROMM), and found the pectoral girdle consistently retracted about 11˚ by rotating caudoventrally about the dorsal scapular processes. This motion occurred mostly after peak gape, so it likely contributed more to accelerating captured prey through the oral cavity and pharynx, than to prey capture as in ray-finned fishes. Our results emphasize the multiple roles of the pectoral girdle in feeding and locomotion, both of which should be considered in studying the functional and evolutionary morphology of this structure.

Introduction

The vertebrate pectoral girdle lies at the boundary between the head and neck, forelimbs, and thorax. Although its structure and evolution have been best studied in the context of locomotion and forelimb function [1, 2], the pectoral girdle also has close connections to the feeding apparatus [3]. Even in tetrapods—where the head is physically and mechanically separated by

the neck—the pectoral girdle is the attachment site for neck, hyoid, and shoulder muscles [2]. The connection between the head and the pectoral girdle is even closer in actinopterygian fishes. In most of these fishes, the pectoral girdle is a multi-jointed structure attached directly to the neurocranium dorsally, while ventrally it is an attachment site for body (hypaxial), hyoid, and pectoral fin muscles [4]. Because of these anatomical connections to the skull, the pectoral girdle is often considered part of the actinopterygian feeding apparatus.

In actinopterygians, pectoral girdle motion can have an important role in suction feeding, which relies on powerful expansion of the buccal cavity to accelerate fluid and food into the mouth. Suction flows are generated by the highly kinetic skull expanding dorsally, laterally, and ventrally as the neurocranium elevates, the suspensoria and opercula abduct, and the hyoid and lower jaw depress [5]. Studies using X-ray video have confirmed that multiple species use hypaxial muscle shortening to retract the pectoral girdle, in turn retracting and depressing the hyoid via hypobranchial muscles [6, 7]. Moreover, in at least largemouth bass the ventral and dorsal body muscles that retract the pectoral girdle and elevate the cranium, respectively, generated over 95% of the power required for suction expansion [8]. Reliance on body muscles may be common among actinopterygian fishes, as the cranial muscles are likely too small to power suction feeding alone. Thus, the pectoral girdle is clearly a dual-function structure in these fishes: supporting the pectoral fins in locomotion, and contributing to mouth expansion and transmitting hypaxial muscle power during suction feeding.

In contrast, dual-function of the pectoral girdle is unclear in sharks as the girdle is completely separated from the skull. Chondrichthyans lack a true neck, but in sharks the pectoral girdle is

displaced caudally (relative to actinopterygians) by the pharyngeal cavity and arches [2] and has no skeletal articulations with the chondrocranium or vertebral column (Fig. 1). Instead, the pectoral girdle is suspended between the epaxial and hypaxial muscles, although it is still the attachment site for hypobranchial muscles [3]. Unlike the jointed, largely dermal girdle of actinopterygians, the pectoral girdle of sharks is a single rigid element covered entirely by muscles and skin—making its motion difficult to measure from external videos commonly used in kinematic studies. Consequently, the pectoral girdle has been studied almost exclusively in locomotion (e.g. [9]) and rarely included in feeding studies.

Suction feeding is used by many sharks, typically benthic-feeding species that expand the mouth cavity primarily by jaw and hyoid depression [10, 11]. Where the pectoral girdle is mentioned, it is hypothesized to be immobile during suction feeding: forming a stable attachment site for the jaw- and hyoid-depressing muscles to shorten against [12], as was proposed for actinopterygian fishes. However, suction-feeding sharks are noted to depress, roll [13], and "perch on" [14] the pectoral fins or push themselves forward over the pectoral girdle [15], demonstrating their ability to finely control pectoral fin—and likely girdle—position. Additionally, studies of actinopterygian suction feeding show pectoral girdle stability is not essential for hyoid depression [6, 7]. Thus, the pectoral girdle of sharks could be mobile and contribute to feeding, despite the anatomical differences compared to ray-finned fishes.

We measured 3D pectoral girdle kinematics in white-spotted bamboo sharks (*Chiloscyllium plagiosum*), using X-ray Reconstruction of Moving Morphology (XROMM). XROMM combines biplanar, high-speed X-ray videos with 3D digital models to generate accurate and

precise animations of *in vivo* skeletal kinematics [16], allowing us to visualize and measure deep structures like the pectoral girdle. Bamboo sharks are benthic, suction-feeding specialists whose feeding morphology, muscle activation, and kinematics are well studied and similar to other suction-feeding sharks [17-19]. We used these XROMM data to investigate 1) whether the pectoral girdle moves relative to the body 2) how the pectoral girdle moves, and 3) the possible role of pectoral girdle motion in suction feeding. Our results show the pectoral girdle is mobile—rotating caudoventrally during suction feeding—but this retraction may have a different function in bamboo sharks than in suction-feeding actinopterygians.

Methods

Three white-spotted bamboo sharks (*Chiloscyllium plagiosum*; SL = 78.6, 79.2, and 85.0 cm for Bam02, Bam03, and Bam04 respectively) were obtained from a reputable supplier. All husbandry and experimental procedures were approved by the Institutional Animal Care and Use Committees of Brown University and the University of Rhode Island. Each shark was anesthetized [18], and at least 3 tungsten carbide conical markers [20] implanted in the chondrocranium, scapulocoracoid (Bam04 only), and left-side palatoquadrate, Meckel's cartilage, and ceratohyal cartilages. Intramuscular markers (0.8 mm tantalum spheres) were implanted in the epaxials (3-6 markers) of all sharks, and the hypaxials (2 markers) of Bam04, following the methods of Camp and Brainerd [6].

Biplanar X-ray videos were recorded of each shark performing at least three suction strikes on pieces of squid or herring (Fig. S1). Two X-ray machines (Imaging Systems and Service, Painesville, OH, USA) generated oblique-view images at 110-120kV and 100mA, which were

recorded at 320-330 frames s^{-1} by Phantom v.10 high-speed cameras (Vision Research, Wayne, NJ, USA). X-ray images of a standard grid and calibration object were also recorded to remove distortion and calibrate the 3D space. Computed-tomography scans (FIDEX CT, Animage, Pleasanton, CA, USA) were taken of each shark (resolution = 416 x 416 or 448 x 448 pixels; slice thickness = 0.185 mm), and mesh models of the cartilages and markers reconstructed in OsiriX (Pixmeo, Geneva, Switzerland) or Horus (horosproject.org) and Geomagic Studio (11, Geomagic, Inc. Triangle Park, NC, USA).

X-ray videos and CT models were combined to create 3D animations of the skeletal kinematics using marker-based XROMM [16] and Scientific Rotoscoping) [21]. For all marked cartilages, marker positions were digitized with a precision of <0.19 mm (calculated as in [16]) and used to calculate the rigid body transformations in XMALab [22], which were then filtered (low-pass Butterworth, 50 Hz cutoff) and applied to animate cartilage models in Maya (2016, Autodesk, San Rafael, CA, USA) using custom scripts and tools (available at xromm.org). A body plane was animated from the motion of the epaxial markers to provide a shark-based frame of reference [6]. For the unmarked scapulocoracoids of Bam02 and Bam03, Scientific Rotoscoping was used in Maya to align the cartilage model to its position in both X-ray images. For each strike, maker-based XROMM and Scientific Rotoscoping were used to create a single XROMM animation of all the cartilages (Fig. S1).

From the XROMM animations, scapulocoracoid and chondrocranium motion was measured relative to the body plane using joint coordinate systems (JCSs). Each JCS described the relative motion of these cartilages as a series of rotations and translations between two anatomical

coordinate systems (ACSs): one attached to the body plane, and one attached to the cartilage of interest [16]. The scapulocoracoid ACSs were placed dorsally and midsagittally so the Z-axis passed through both suprascapular processes and the Y-axis was parallel to the scapula (Fig. 2A). The chondrocranium ACSs were placed at the craniovertebral joint with the X-axis running midsagittally (Fig. S2A). For both cartilages, the X-axis described rostrocaudal translation and long-axis rotation, the Y-axis described dorsoventral translation and mediolateral rotation, and the Z-axis described transverse translation and elevation-depression (chondrocranium) or protraction-retraction (scapulocoracoid) rotations (Fig. 2A-C, Fig. S2). We also measured the 3D displacements of virtual markers on the ventral, midsagittal keel of the scapulocoracoid and the ventral tip of the ceratohyal, relative to an ACS fixed to the body plane (Fig. 3A). Again, rostrocaudal translations were described by the X-axis, dorsoventral by the Y-axis, and transverse by the Z-axis. Virtual markers on the rostral tips of the palatoquadrate and Meckel's cartilage were used to measure gape distance.

Hypaxial muscle length was measured in Bam04 with fluoromicrometry: using biplanar X-ray video to measure the change in distance between intramuscular markers [23]. These markers were placed directly caudal to the pectoral girdle, to measure hypaxial length changes near its insertion on the coracoid bar, in a craniocaudal series approximately parallel to the fiber orientation of the hypaxials. Intramuscular markers were digitized in XMALab, and their 3D positions used to calculate muscle length and strain with a custom script in MATLAB (R2015a, The Mathworks, Natick, USA). Hypaxial length was measured over three regions (Fig. 4A): between the two hypaxial markers ($L_{HP\text{-}post}$), from the scapulocoracoid virtual marker to the anterior hypaxial marker ($L_{HP\text{-}ant}$), and from the scapulocoracoid virtual marker to the posterior

hypaxial marker ($L_{HP\text{-}total}$). Muscle strain was calculated as the change in length from the initial length (at 400 ms prior to peak gape) divided by initial length, with positive strain indicating muscle lengthening, and negative strain indicating muscle shortening.

The mean magnitude of peak skeletal excursions from the JCSs and virtual markers were calculated for each individual, as the three sharks showed distinct kinematic patterns. A total of 11 strikes were analyzed (4 from Bam02, 4 from Bam03, and 3 from Bam04), using a custom script in MATLAB. Time was calculated relative to the time of peak gape (time zero), and we examined all variables from 400 ms prior to peak gape, to 200 ms after peak gape. All kinematic variables were calculated relative to their initial values at -400 ms.

Results

All sharks captured prey with suction: rapidly opening the jaws and depressing the hyoid to accelerate food into the mouth. However, the kinematics varied considerably within and among individuals as previously observed in this species [18]. Therefore, we report individual means and standard errors ($N = 4$ for Bam02 and Bam 03; $N = 3$ for Bam04) below and in Table 1.

All sharks consistently retracted the scapulocoracoid (rotated caudoventrally about the Z-axis) relative to the body plane (Movie S1). In Bam02 and 04, the scapulocoracoid initially protracted (rotated rostrodorsally about the Z-axis) by a mean of 6.2 (±1.6)° and 3.9 (±0.5)° before retracting (Fig. 2D). Peak scapulocoracoid retraction, i.e., the change in Z-axis rotation from peak protraction to peak retraction, averaged 11° for all individuals (Table 1). Scapulocoracoid protraction, when present, occurred as the jaws opened, while scapulocoracoid retraction began

182 just before peak gape and reached its peak at a mean of 151 (±31), 123 (±26), and 133 (±3) ms
183 after peak gape for Bam01, Bam02, and Bam03, respectively (Fig. 2D). Rotations of the
184 scapulocoracoid about the X-axis (roll) and Y-axis (yaw) relative to the body plane varied
185 greatly in Bam02 and Bam03 (Table 1), likely reflecting differences in body posture across
186 strikes. Bam04 had small, but consistent anti-clockwise roll (mean peak of 2.3 ± 0.2°, when
187 viewed from the head) and yaw to the right (mean peak of -1.6 ± 0.2°).
188
189 The scapulocoracoid translated very little relative to the body plane (Fig. 2C), even though this
190 cartilage is suspended in muscle. Translations along all axes of the JCS were small (< 4 mm) and
191 highly variable in Bam02 and 03 (Table 1), again suggesting differences in body posture. Only
192 Bam04 showed consistent translations dorsally and to the left (Fig. 2C), but these were quite
193 small (mean peak translation < 1 mm). Thus, the motion of the scapulocoracoid could be
194 described almost entirely by rotation about a transverse axis passing through both dorsal scapular
195 processes (Z-axis, Fig. 2).
196
197 Scapulocoracoid retraction displaced the coracoid bar caudally and ventrally, as measured by the
198 motion of a virtual marker relative to the body plane (Fig. 3). Across all sharks, the mean peak
199 displacement was at least 5 mm caudally and 2 mm ventrally (Table 1) and occurred mostly or
200 wholly during gape closing (Fig. 3B-D). The ceratohyal also moved caudally and ventrally
201 relative to the body plane, but its displacement was 2-3 times greater (mean peaks of at least 15
202 mm caudally and 10 mm ventrally), and peak displacements were reached just after peak gape
203 (Fig. 3D). The mean times of peak caudal and ventral ceratohyal displacements were at least 70
204 ms earlier than those of the coracoid in all individuals. Where protraction was present, the

coracoid and ceratohyal moved rostrally and dorsally as the gape opened (Fig. 3C), although peak magnitudes were generally higher in the coracoid (Table 1).

Hypaxial muscle shortened during scapulocoracoid retraction in Bam04, however the total region measured ($L_{HP\text{-}total}$) showed a different strain pattern from the anterior and posterior sub-regions ($L_{HP\text{-}ant}$ and $L_{HP\text{-}post}$). Measured from the coracoid marker to the posterior hypaxial marker, $L_{HP\text{-}total}$ remained nearly isometric during scapulocoracoid protraction and shortened (mean peak of -6.5 ± 0.7%) as the scapulocoracoid retracted (Fig. 4B). In contrast, $L_{HP\text{-}ant}$ lengthened (mean peak of 3.1 ± 1.2%) during scapulocoracoid protraction, and shortened (mean peak of -6.8 ± 0.5%) during retraction, while $L_{HP\text{-}post}$ shortened (mean peak of -13.9 ± 0.9%) mostly during scapulocoracoid protraction and began re-lengthening as the scapulocoracoid was retracting (Fig. 4B).

We also measured chondrocranium motion relative to the body plane, but only Bam04 showed consistent chondrocranium elevation (mean peak of 4.9 ± 1.1° rostrodorsal rotation about the Z-axis), which occurred after peak gape (Fig. S2). Chondrocranium motions in Bam02 and 03 were much smaller and more variable (Table S1). As expected, translations of the chondrocranium relative to the body plane were quite small (<1 mm, Table S1).

Discussion

The pectoral girdle consistently retracts during suction feeding in bamboo sharks, a motion driven by hypaxial muscle shortening and achieved almost entirely by caudoventral rotation about a transverse axis. The scapulocoracoid moves as though rotating about joints at the

suprascapular processes, even though it is suspended between the body muscles. These pectoral girdle kinematics are similar to those of actinopterygian fishes during suction feeding, but likely serve a different role. Pectoral girdle retraction in actinopterygians contributes to accelerating food into the mouth, but in bamboo sharks it occurs almost entirely after peak gape and more likely generates flows within the oral cavity to keep captured prey moving through the pharyngeal cavity and towards the esophagus.

This study is the first direct measurement of the pectoral girdle moving and contributing to suction feeding in a shark. The pectoral girdle has been hypothesized to remain stationary during feeding in sharks, providing a stable attachment site for the jaw- and hyoid-depressing muscles to shorten against [3, 12, 15, 24]. In contrast, we found the pectoral girdle moved as these muscles shortened: protracting as the hyoid elevated during the preparatory phase (when present), and then retracting during hyoid depression (Fig. 3). A stable pectoral girdle, therefore, is not required for the hypobranchial muscles to generate hyoid and jaw depression in sharks [17, 18]. While this study only examined white-spotted bamboo sharks, their pectoral girdle morphology, feeding kinematics, and suction performance are similar to other suction-feeding sharks [14, 15, 25]. Thus, we expect pectoral girdle motion is common in suction-feeding sharks, although additional studies are needed to confirm this.

Scapulocoracoid retraction is achieved by rotation about a single axis, despite the lack of any skeletal articulation. Without joints to constrain its motion, the pectoral girdle might be expected to translate rather than rotate as it retracts relative to the body. However, pectoral girdle motion could be described almost entirely by rotation about a transverse axis through the suprascapular

processes (Fig. 2, Movie S1), with negligible translations (generally <3 mm for these 80 cm long sharks). We propose this rotation is the product of hypaxial muscles shortening to pull the scapulocoracoid caudally (Figs. 3-4), while active force production in the epaxials and cucullaris resist translations and stabilize the dorsal scapulae and suprascapular processes. Previous studies have confirmed that the epaxials are active during suction feeding in this species [17], despite very little motion of the chondrocranium especially when feeding off the substrate (Fig. S2, also [11, 18]. The dorsal scapulae and suprascapular processes could also be passively stabilized by expaxial musculature and myosepta, or by connective tissue attachments to the skin. Any of these mechanisms would allow pectoral girdle rotation in the absence of skeletal articulations with the vertebral column or skull.

While the pectoral girdle retracted during every strike we measured, in Bam02 and Bam04 it first protracted (Movie S1). This protraction did not change the total caudoventral retraction of the pectoral girdle (mean peak of 11° for all sharks, Table 1), but may be part of a preparatory phase together with ceratohyal elevation. We suggest the pectoral girdle was protracted by the coracohyoid and coracoarcualis muscles as the ceratohyal elevated, and then retracted by the hypaxial muscles during rapid ceratohyal depression and retraction (Fig. 3). In Bam04, hypaxial shortening began during pectoral girdle protraction, resulting in lengthening in the anterior hypaxials while the posterior hypaxials shortened (Fig. 4C). This strain heterogeneity suggests the preparatory phase prevented pectoral girdle retraction until the ceratohyal also began retracting, presumably as a result of coracohyoid and coracoarcualis muscle shortening. The preparatory phase may decrease initial mouth volume to increase the rate of volume change—and therefore flow velocity—during suction feeding, although clearly it is not essential as it was

absent in Bam03. Alternatively, the preparatory phase observed in this study may be part of an elastic energy storage and power amplification mechanism that has been proposed for this species based on measurements of length and activation of the coracoarcualis and coracohyoid muscles during suction feeding [17].

Pectoral girdle retraction in bamboo sharks is similar to that of some actinopterygian fishes, but the role of these motions in suction feeding likely differs between the two groups. Like the shark scapulocoracoid, the cleithrum in some actinopterygians is rotated caudoventrally (retracted) by the hypaxial muscles during suction feeding [6, 26], generating hyoid depression and retraction and contributing to the rapid buccal cavity expansion that accelerates water and food into the mouth. Scapulocoracoid retraction in bamboo sharks likely contributes little to capturing prey, as the majority of retraction occurs as the mouth is closing and peak retraction is about 70 ms later than peak hyoid motion (Fig. 3). However, because the pectoral girdle is positioned quite far posterior to the cranium (Fig. 1) compared to actinopterygians, its retraction may be key to accelerating captured prey through the relatively long pharynx by continuing the anterior-to-posterior wave of expansion. While pectoral girdle retraction may also contribute to hyoid depression in bamboo sharks, the delay between peak hyoid and scapulocoracoid retraction suggests hypaxial muscles are unlikely to be a major source of suction power as in some actinopterygians [8]. Like upper jaw protrusion and cranial elevation [10, 11, 25], pectoral girdle motion is similar in sharks and actinopterygians, but serves different roles in these two groups.

Our measurements of chondrocranium kinematics confirmed the results of previous external-video studies: suction-feeding sharks exhibit little cranial elevation when feeding benthically on

297 non-elusive prey. Only Bam04 showed consistent cranial elevation of about 5˚ relative to the
298 body plane, while Bam02 and Bam03 generally had smaller magnitude motions that included
299 both elevation and depression. While cranial elevation might be slightly greater and/or more
300 consistent during pelagic prey capture, suction feeding sharks often use little cranial motion [14,
301 15, but see 27] especially compared to actinopterygians where neurocranium elevation is a major
302 contributor to suction feeding [5].
303
304 Our results emphasize the dual-function of the pectoral girdle for locomotion and feeding in
305 sharks and actinopterygian fishes, and suggest that both functions may have shaped its evolution.
306 Even an immobile pectoral girdle functions in feeding as an attachment site for hyoid and/or
307 neck muscles across gnathostomes, yet much of the work on the origin and function of the
308 pectoral girdle in fishes has focused exclusively on its locomotor role in limb support and motion
309 [2]. We now have evidence that pectoral girdle retraction can contribute to buccal cavity
310 expansion during suction feeding in both chondrichthyan and actinopterygian [6, 7] fishes.
311 Finding pectoral girdle retraction in these sharks was surprising given the tetrapod-like
312 separation of the girdle from the chondrocranium; clearly an articulation with the skull is not
313 necessary for pectoral girdle kinematics to contribute to feeding. In actinopterygians, pectoral
314 girdle retraction allows the hypaxial muscles to actively shorten and contribute power for suction
315 feeding [6]. However, pectoral girdle retraction in bamboo sharks seems to function primarily to
316 transport prey within the mouth cavity and may be part of a “hydrodynamic tongue”: the
317 generation of fluid flows to move and reorient food within the mouth [28, 29]. Thus, we expect
318 the pectoral girdle also retracts during prey transport in bamboo sharks. Ram- or bite-feeding

fishes may also use pectoral girdle retraction to expand the mouth cavity when engulfing prey, and/or to transport captured prey using "hydraulic suction" [10].

There are few data on pectoral girdle motion during swimming or body support in sharks, making it difficult to compare feeding- and locomotion-based kinematics. As in feeding studies, the girdle is often assumed to be a stable attachment site for the pectoral fin muscles and skeleton (e.g., [9]). A study of submerged walking in a shark found that the girdle rotates about a dorsoventral axis (yaw) [30] instead of about a mediolateral axis (retraction) as we saw during feeding. Thus, mobility of the pectoral girdle (relative to the body) may be important for both its functions. Pectoral fin motion was not visible in our X-ray videos, but during filming we observed the sharks using their fins to position themselves over the prey, as in previous studies [13-15]. These observations suggest that the pectoral girdle may perform feeding and locomotor roles simultaneously in bamboo sharks. Additional studies of pectoral girdle kinematics in extant cartilaginous and ray-finned fishes are needed to understand how both roles have shaped the evolution of this structure, and what morphological features are correlated with its functions in feeding and locomotion.

Data accessibility

The XROMM animations used in this study are available on the X-ray Motion Analysis Portal (xmaportal.org, Study Identifier URI1).

Author contributions

ELB, CDW, and ALC designed the study. ELB, CDW, and BS collected X-ray video and CT scan data, and ALC and BS generated XROMM animations. ALC analyzed the data and drafted the manuscript. All authors contributed to editing the manuscript and approved the final version.

Competing interests

We declare we have no competing interests.

Funding

This research was supported by National Science Foundation (NSF) grants awarded to ELB (1655756) and CDW (IOS 1354189, 1631165).

Acknowledgements

We are grateful to Erika Giblin for assistance with X-ray filming experiments, and to Laura Vigil, Ben Concepcion, and Preston Steele for providing shark husbandry and training.

References

1. Shubin N.H., Daeschler E.B., Jenkins F.A. 2006 The pectoral fin of Tiktaalik roseae and the origin of the tetrapod limb. *Nature* **440**(7085), 764-771. (doi:10.1038/nature04637).
2. McGonnell I.M. 2001 The evolution of the pectoral girdle. *J Anat* **1999**, 189-194.
3. Gudo M., Homberger D.G. 2002 The functional morphology of the pectoral fin girdle of the Spiny Dogfish (Squalus acanthias): Implications for the evolutionary history of the pectoral girdle of vertebrates. *Senckenb Lethaea* **82**(1), 241-252. (doi:10.1007/bf03043787).
4. Gosline J. 1977 The structure and function of the dermal pectoral girdle in bony fishes with particular reference to ostariophysines. *J Zool, Lond*.
5. Lauder G.V. 1985 Aquatic feeding in lower vertebrates. In *Functional Vertebrate Morphology* (eds. Hildebrand M., DM B., Liem K., DB W.), pp. 185-229. Cambridge, MA, Harvard Univ Press.

6. Camp A.L., Brainerd E.L. 2014 Role of axial muscles in powering mouth expansion during suction feeding in largemouth bass (*Micropterus salmoides*). *J Exp Biol* **217**(8), 1333-1345. (doi:Doi 10.1242/Jeb.095810).
7. Van Wassenbergh S., Herrel A., Adriaens D., Aerts P. 2005 A test of mouth-opening and hyoid-depression mechanisms during prey capture in a catfish using high-speed cineradiography. *J Exp Biol* **208**(Pt 24), 4627-4639. (doi:10.1242/jeb.01919).
8. Camp A.L., Roberts T.J., Brainerd E.L. 2015 Swimming muscles power suction feeding in largemouth bass. *Proc Natl Acad Sci U S A* **112**(28), 8690-8695. (doi:10.1073/pnas.1508055112).
9. Wilga C.D., Lauder G.V. 2001 Functional morphology of the pectoral fins in bamboo sharks, *Chiloscyllium plagiosum*: Benthic vs. Pelagic station-holding. *J Morphol* **249**, 195-209.
10. Motta P.J., Wilga C.D. 2001 Advances in the study of feeding behaviors, mechanisms, and mechanics of sharks. *Environ Biol Fishes* **60**, 131-156.
11. Wilga C.D., Motta P.J., Sanford C.P. 2007 Evolution and ecology of feeding in elasmobranchs. *Integr Comp Biol* **47**(1), 55-60.
12. Wilga C., Wainwright P., Motta P. 2000 Evolution of jaw depression mechanics in aquatic vertebrates: insights from Chondrichthyes. *Biol J Linn Soc* **71**(1), 165-185.
13. Moss S. 1972 Nurse shark pectoral fins: an unusual use. *Am Midl Nat* **88**(2), 496-497.
14. Ajemian M.J., Sanford C.P. 2007 Food capture kinematics in the deep-water chain catshark Scyliorhinus retifer. *Journal of the Marine Biological Association of the UK* **87**(05). (doi:10.1017/s0025315407055701).
15. Wu E. 1994 Kinematic analysis of jaw protrusion in orectolobiform sharks: a new mechanism for jaw protrusion in elasmobranchs. *J Morphol* **222**(2), 175-190.
16. Brainerd E.L., Baier D.B., Gatesy S.M., Hedrick T.L., Metzger K.A., Gilbert S.L., Crisco J.J. 2010 X-ray reconstruction of moving morphology (XROMM): precision, accuracy and applications in comparative biomechanics research. *J Exp Zool* **313A**(5), 262-279. (doi:10.1002/jez.589).
17. Ramsay J.B. 2012 A comparative investigation of cranial morphology, mechanics, and muscle function in suction and bite feeding sharks, University of Rhode Island.
18. Wilga C.D., Sanford C.P. 2008 Suction generation in white-spotted bamboo sharks Chiloscyllium plagiosum. *J Exp Biol* **211**(Pt 19), 3128-3138. (doi:10.1242/jeb.018002).
19. Nauwelaerts S., Wilga C.D., Lauder G.V., Sanford C.P. 2008 Fluid dynamics of feeding behaviour in white-spotted bamboo sharks. *J Exp Biol* **211**(Pt 19), 3095-3102. (doi:10.1242/jeb.019059).
20. Kambic R.E., Roberts T.J., Gatesy S.M. 2014 Long-axis rotation: a missing degree of freedom in avian bipedal locomotion. *J Exp Biol* **217**(Pt 15), 2770-2782. (doi:10.1242/jeb.101428).
21. Gatesy S.M., Baier D.B., Jenkins F.A., Dial K.P. 2010 Scientific rotoscoping: a morphology-based method of 3-D motion analysis and visualization. *J Exp Zool* **313**(5), 244-261.
22. Knorlein B.J., Baier D.B., Gatesy S.M., Laurence-Chasen J.D., Brainerd E.L. 2016 Validation of XMALab software for marker-based XROMM. *J Exp Biol* **219**(Pt 23), 3701-3711. (doi:10.1242/jeb.145383).
23. Camp A.L., Astley H.C., Horner A.M., Roberts T.J., Brainerd E.L. 2016 Fluoromicrometry: a method for measuring muscle length dynamics with biplanar videofluoroscopy. *Journal of Experimental Zoology, Part A* **325A**, 399-408.

24. Motta P., Tricas T., Hueter… R. 1997 Feeding mechanism and functional morphology of the jaws of the lemon shark Negaprion brevirostris (Chondrichthyes, Carcharhinidae). *J Exp Biol*.
25. Motta P.J., Hueter R.E., Tricas T.C., Summers A.P., Huber D.R., Lowry D., Mara K.R., Matott M.P., Whitenack L.B., Wintzer A.P. 2008 Functional morphology of the feeding apparatus, feeding constraints, and suction performance in the nurse shark Ginglymostoma cirratum. *J Morphol* **269**(9).
26. Van Wassenbergh S., Herrel A., Adriaens D., Aerts P. 2007 Interspecific variation in sternohyoideus muscle morphology in clariid catfishes: functional implications for suction feeding. *J Morphol* **268**(3), 232-242. (doi:10.1002/jmor.10510).
27. Matott M., Motta P., Hueter R. 2005 Modulation in feeding kinematics and motor pattern of the nurse shark Ginglymostoma cirratum. *Environ Biol Fishes*.
28. Bemis W., Lauder G.V. 1986 Morphology and function of the feeding apparatus of the lungfish, Lepidosiren paradoxa (Dipnoi). *J Morphol* **187**(1), 81-108.
29. Dean M.N., Wilga C.D., Summers A.P. 2005 Eating without hands or tongue: specialization, elaboration and the evolution of prey processing mechanisms in cartilaginous fishes. *Biol Lett* **1**(3), 357-361. (doi:10.1098/rsbl.2005.0319).
30. Pridmore P.A. 1994 Submerged walking in the epaulette shark *Hemiscyllium ocellatum* (Hemiscyllidae) and its implications for locomotion in rhipidistian fishes and early tetrapods. *Zoology* **98**, 278-297.

Table and Figure Captions

Table 1: Mean and standard error of peak magnitudes of skeletal rotations (rot.) in °, translations (trans.) and displacements (disp.) in mm, and hypaxial muscle strain (%).

	Motion	Bam02 *N* = 4	Bam03 *N* = 4	Bam04 *N* = 3
Scapulocoracoid	Roll (X rot.)	-6.8 (2.0)	-4.9 (2.8)	2.3 (0.2)
	Pitch (Y rot.)	-2.7 (1.1)	-0.9 (0.4)	-1.6 (0.2)
	Protraction (+Z rot.)	6.3 (1.6)	1.0 (0.6)	3.9 (0.5)
	Retraction (-Z rot.)	-5.5 (2.0)	-10.0 (1.2)	-7.1 (0.8)
	Rostrocaudal trans. (X)	-1.3 (0.4)	-1.7 (0.8)	-0.3 (0.0)
	Dorsoventral trans. (Y)	1.9 (0.9)	1.3 (0.6)	0.6 (0.0)
	Transverse trans. (Z)	-2.8 (0.4)	-0.8 (0.5)	-0.5 (0.1)
Coracoid virtual marker	Rostral disp. (+X)	3.9 (1.3)	1.2 (0.6)	2.8 (0.5)
	Caudal disp. (-X)	-5.3 (1.9)	-7.5 (0.7)	-5.9 (0.6)
	Dorsal disp. (+Y)	3.2 (1.2)	0.3 (0.2)	2.4 (0.3)
	Ventral disp. (-Y)	-1.9 (1.3)	-6.7(1.2)	-2.9 (0.3)
Ceratohyal virtual marker	Rostral disp. (+X)	0.2 (0.2)	0.0 (0.0)	0.1 (0.0)
	Caudal disp. (-X)	-14.7 (2.3)	-15.8 (0.9)	-14.8 (0.6)
	Dorsal disp. (+Y)	1.1 (0.7)	0.1 (0.1)	1.3 (0.8)
	Ventral disp. (-Y)	-9.8 (2.4)	-15.2 (1.0)	-9.8 (0.6)
Hypaxial strain	$L_{HP\text{-}ant}$ total strain	-	-	9.9 (0.8)
	$L_{HP\text{-}post}$ total strain	-	-	15.5 (1.9)
	$L_{HP\text{-}total}$ total strain	-	-	7.3 (0.2)

444 **Figure 1**. Cartilages (black) and muscles (red) of the feeding apparatus in white-spotted bamboo
445 sharks, with myosepta orientation shown for segmented muscles. The coracoid bar, scapulae, and
446 suprascapular processes together form the scapulocoracoid. The coracomandibularis is omitted
447 for clarity.
448
449
450 **Figure 2**. Kinematics of the scapulocoracoid, measured relative to the body plane. A joint
451 coordinate system (**A**) measured rotations (**B**) and translations (**C**) about each axis (data from a
452 sample strike). (**D**) Z-axis rotations of the scapulocoracoid from each strike (blue lines), and the
453 mean rotation at each time step (black line), for each individual. Time is calculated relative to the
454 time of peak gape.
455
456 **Figure 3**. Displacement of ceratohyal and coracoid bar virtual markers, relative to an anatomical
457 coordinate system attached to the body plane (**A**). Sample data from two Bam03 strikes, with (**B**)
458 and without (**C**) protraction, showing rostrocaudal and dorsoventral displacements of each
459 marker and gape distance (dashed line). For each shark, mean displacements at each time step
460 (**D**) are shown with standard error bars ($N = 3$ or 4 strikes for each shark). Time is calculated
461 relative to the time of peak gape (vertical dashed line).
462
463 **Figure 4.** Hypaxial muscle length during three strikes from Bam04. (**A**) Lateral view of muscle
464 markers and lengths measured over three regions: the coracoid marker to the posterior
465 intramuscular marker (grey, $L_{HP\text{-}total}$), the coracoid marker to the anterior intramuscular marker
466 (red, $L_{HP\text{-}ant}$), and between the intramuscular markers (black, $L_{HP\text{-}post}$). (**B**) Scapulocoracoid Z-

axis rotation, with the duration of retraction highlighted in blue. (**C**) Hypaxial strain, relative to initial length, of each region. Time is calculated relative to the time of peak gape.

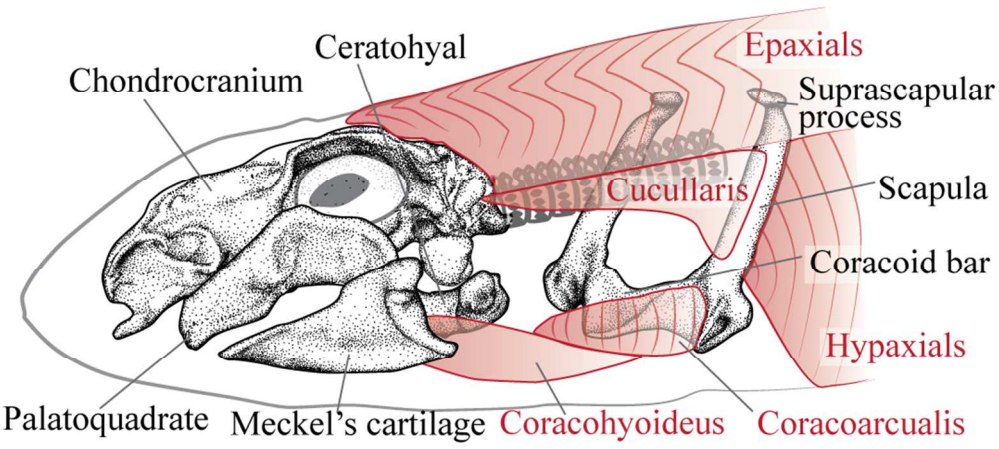

Figure 1. Cartilages (black) and muscles (red) of the feeding apparatus in white-spotted bamboo sharks, with myosepta orientation shown for segmented muscles. The coracoid bar, scapulae, and suprascapular processes together form the scapulocoracoid. The coracomandibularis is omitted for clarity.

91x40mm (300 x 300 DPI)

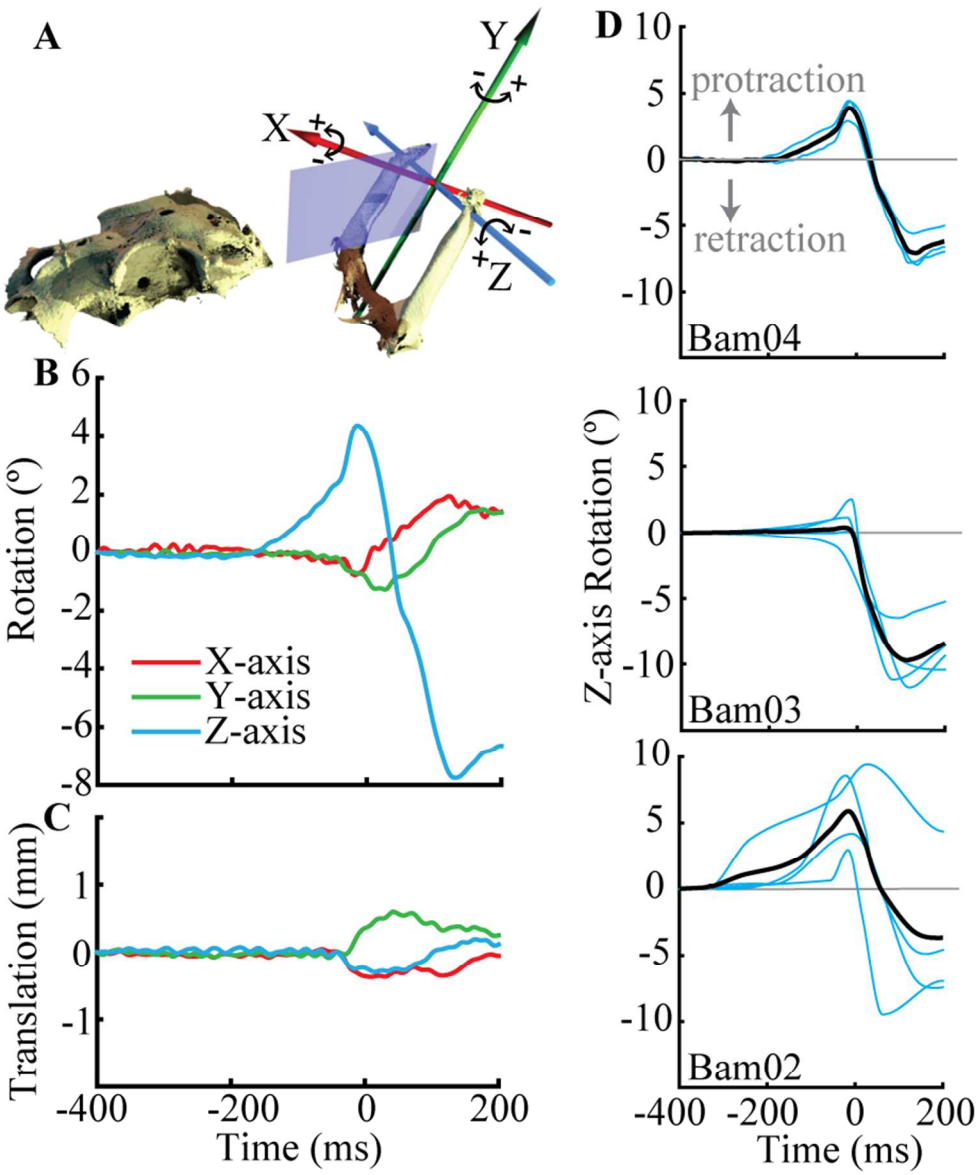

Figure 2. Kinematics of the scapulocoracoid, measured relative to the body plane. A joint coordinate system (A) measured rotations (B) and translations (C) about each axis (data from a sample strike). (D) Z-axis rotations of the scapulocoracoid from each strike (blue lines), and the mean rotation at each time step (black line), for each individual. Time is calculated relative to the time of peak gape.

79x93mm (300 x 300 DPI)

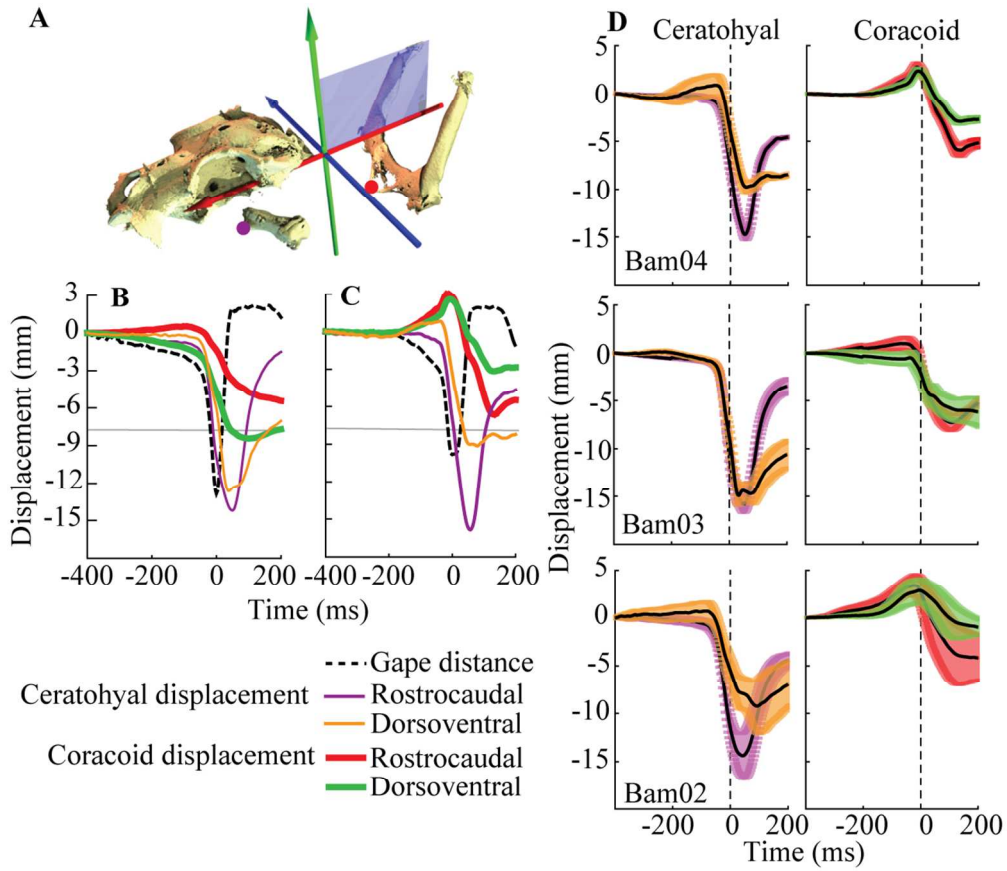

Figure 3. Displacement of ceratohyal and coracoid bar virtual markers, relative to an anatomical coordinate system attached to the body plane (A). Sample data from two Bam03 strikes, with (B) and without (C) protraction, showing rostrocaudal and dorsoventral displacements of each marker and gape distance (dashed line). For each shark, mean displacements at each time step (D) are shown with standard error bars (N = 3 or 4 strikes for each shark). Time is calculated relative to the time of peak gape (vertical dashed line).

109x95mm (300 x 300 DPI)

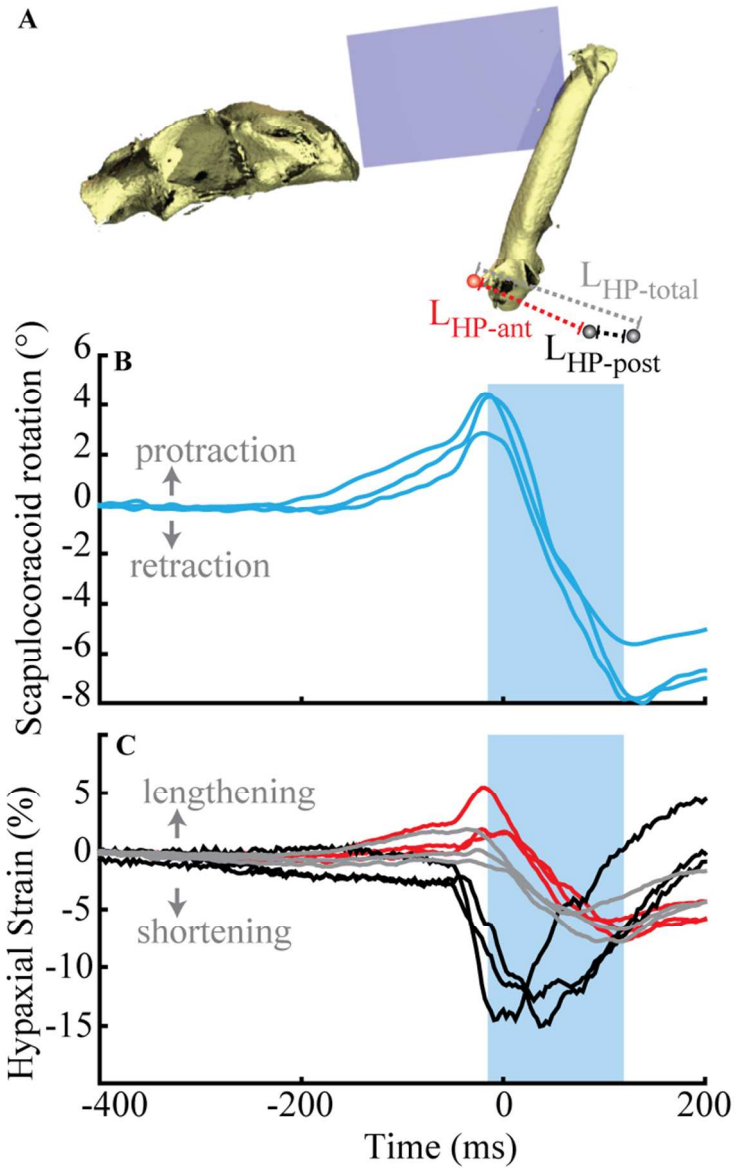

Figure 4. Hypaxial muscle length during three strikes from Bam04. (A) Lateral view of muscle markers and lengths measured over three regions: the coracoid marker to the posterior intramuscular marker (grey, LHP-total), the coracoid marker to the anterior intramuscular marker (red, LHP-ant), and between the intramuscular markers (black, LHP-post). (B) Scapulocoracoid Z-axis rotation, with the duration of retraction highlighted in blue. (C) Hypaxial strain, relative to initial length, of each region. Time is calculated relative to the time of peak gape.

64x103mm (300 x 300 DPI)